18. V. Yu. Zaichenko, L. V. Kuznetsova, and V. M. Tyul'tev, "Study of the stress state of a rock mass by the method of acoustic logging when the medium is acted upon by an explosion," in: Study of the Stress State of Rock Masses by the Acoustic Method [in Russian], VNIIYaGG, Moscow (1980).

REACTION OF A THREE-LAYER HYDROELASTIC CYLINDRICAL SHELL TO AN AXISYMMETRIC INTERNAL EXPLOSION

A. I. Belov, V. A. Kornilo,
N. I. Pinchukova, and M. V. Stepanenko

UDC 539.3

A relatively small number of publications has been devoted to the experimental study of the elastic deformation of shells under explosive loading. The first studies in this area [1-3] examined the dynamics of closed metal shells to obtain estimates of the strength of blast chambers. The status of these investigations was analyzed in [4] and a fairly complete survey of the literature was made. It was apparent from the survey that most of the studies examined the dynamics of one-layer shells with a monolithic wall. It was shown (in [4, 5], for example) that the dynamic reaction of the shell depends not only on the energy released by the explosion but on features of the natural vibration-frequency spectrum of structures. In particular, an increase in the amplitude of the vibrations ("buildup") was noted. In the opinion of the authors, this phenomenon is due to interaction of natural modes of vibration and it leads to a significant increase in shell deformation compared to the strains calculated on the basis of the simplest model of a shell as a system with one degree of freedom.

There is almost no data on the dynamics of elastic shells with a more complicated structure, such as multilayer shells with a combination of dissimilar materials. Results were presented in [8] from an experiment with a three-layer shell subjected to shock loading. The dependence of the strain of the external layer on the parameters of the filler material was determined. The inside and outside layers of the shell were made of steel, while the material of the intervening layer was varied — water, sand, or concrete (only data on the amplitudes of the maximum strains was presented, and no information was given on features of the vibration process).

Here we study the dynamics of a three-layer (metal—liquid—metal) shell loaded by the detonation of a linear explosive charge on the axis. The study is conducted within the elastic range of deformation of the bearing layers. We determine the dependence of the shell strains on the thickness of the liquid layer and obtain data on features of the vibration process which develops in the system.

The test model (Fig. 1) consisted of two cylindrical shells 1 and 2. The space between the shells was filled with water 3. The model was loaded by the detonation of an explosive charge 4 in air. The charge was placed along the geometric axis of the system. The internal cavity and the annular volume between the shells were enclosed by flat monolithic heads 5. The joint between the cylindrical shells and flanges corresponded structurally to a scheme of rigid fastening. The thickness of the layer of liquid filler H was changed gradually by replacing the external shells. The number of values of H studied was not large, which had to do with technical difficulties. As a result, the range of thicknesses was chosen to be rather large: $H/R_1 = 0.23$-0.66 (R_1 and R_2 are the radii of the internal and external layers). The shells were made of flat-rolled steel Kh18N10T of the thickness $h_1 = h_3 = 3$ mm and had the following dimensions: $D_1 = 234$ mm, $D_2 = 294$, 334, and 394 mm; length $L = 1200$ mm. The chosen dimensions of the system made it possible to prevent the strains measured in sections L/2 from being affected by perturbations reflected from the ends (at least during the first half-period of the circumferential vibrations). We used linear charges with the same weight of explosive. The charges consisted of three tightly packed detonating fuses of the DSh-A type (detonation velocity $v_D = 6500$ m/sec, the explosive was pentaerythrityl tetranitrate, and the linear weight of explosive for one fuse was $1.2 \cdot 10^{-2}$ kg/m). The charge was detonated from one end. The arrow in Fig. 1 denotes the direction of propagation of the detonation wave.

Novosibirsk. Translated from Zhurnal Prikladnoi Mekhaniki i Tekhnicheskoi Fiziki, No. 1, pp. 152-157, January-February, 1986. Original article submitted December 7, 1984.

0021-8944/86/2701-0139$12.50

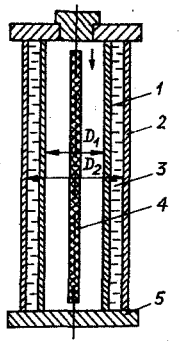

Fig. 1

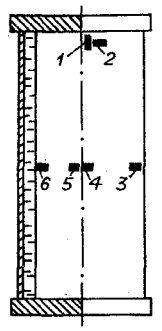

Fig. 2

The experiment involved measurement of the pressures on the walls and the strains of the outside surfaces of the bearing layers. Strains were measured with commercial PKP-10-100 strain gauges. A diagram showing the location of the gauges on the shell is presented in Fig. 2. The gauges were connected to a measurement circuit in a half-bridge (potentiometric) scheme. No temperature compensation was provided due to the relative brevity of the process. An electric analog of the strains was recorded with S8-13 cathode-ray oscillographs. The system which measured pressure include: a vibration-compensated piezoelectric pressure transducer with a quartz sensitive element, a preamplifier, and an S8-13 oscillograph. The lower level of the natural frequencies of the transducer was about 180 kHz, while the sensitivity to acceleration was no more than 10 Pa/g. The transmission band of the preamp was 0-150 kHz, and the drop in the amplitude–frequency characteristic was 80 dB/sec. We also measured the pressure in a shock wave acting on a shell with a monolithic wall and a geometry corresponding to the internal cavity of the three-layer shell. The transducer was secured in section L/2. The sensitive surface of the transducer was oriented toward the center of the shell and was placed at the level of the inside surface of the latter. The level of the signals from the transducer caused by acceleration of its body as it moved with the shell wall did not exceed 10^{-1} MPa (about 1% of the pressure at the shock front).

The results presented below were obtained by statistical analysis of a series of experiments. Seven to 15 tests were conducted in each experiment, which ensured an acceptable level of measurement error (no greater than 10–15%). The confidence intervals of the quantities were determined for a confidence level P = 0.95 (with respect to pressure) and P = 0.9 (with respect to strain).

We tried to make the shell strain as close to unidimensional as possible by proper selection of the geometry of the charge and shell. This allowed us to simplify the subsequent interpretation of the results, impart a large measure of generality to the phenomena investigated, and measure mainly circumferential strains in the central part of the shell (gauges 3-6). The stress–strain state was close to being uniaxial during the first half-period of shell vibration since the measured amplitudes of the axial strains in this time interval were significantly lower than the amplitudes of the circumferential strains.

Figure 3 shows typical oscillograms of pressure on the inside surface of the shell wall with the explosion of an axisymmetrically-positioned charge consisting of three filaments of explosive DSh. The presence of axial symmetry in the system results in a series of periodic pressure pulses caused by the successive reflection of an air shock wave from the inside surface of the wall and its collapse in the center of the shell. In most of the experiments the amplitudes of the secondary shock waves decayed with time (Fig. 3b).

The values of the measured shock-wave parameters were as follows:

$$p_0 = 16 \text{ MPa}, \ \tau_0 = 82 \cdot 10^{-6} \text{ sec}, \ I = 400 \text{ N} \cdot \text{sec/m}^2,$$
$$\delta(p_0) = 3{,}8 \text{ MPa}, \ \delta(\tau_0) = 26 \cdot 10^{-6} \text{ sec}, \ \delta(I) = 66 \text{ N} \cdot \text{sec/m}^2.$$

Here, p_0 is the total pressure on the front in the forward-traveling and reflected shock waves; τ_0 is the characteristic time of action of the impulse (determined as the time over which pressure decreased by a factor of 10); I is the impulse of the shock wave (obtained by integrating the pressure oscillograms); $\delta(\ldots)$ are confidence intervals.

Figure 4a–c shows typical strain oscillograms for H = 27, 47, and 77 mm, respectively (the inside layer is on the left and the outside layer is on the right). Table 1 shows values of the peak amplitudes of the circumferential strains in the bearing layers of the shell for

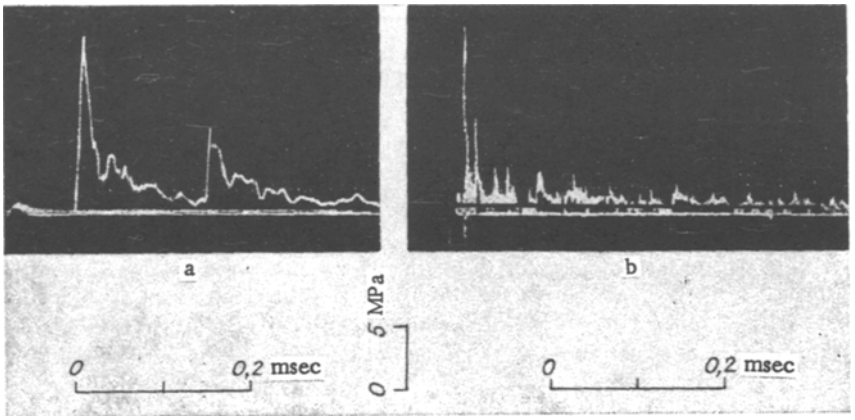

Fig. 3

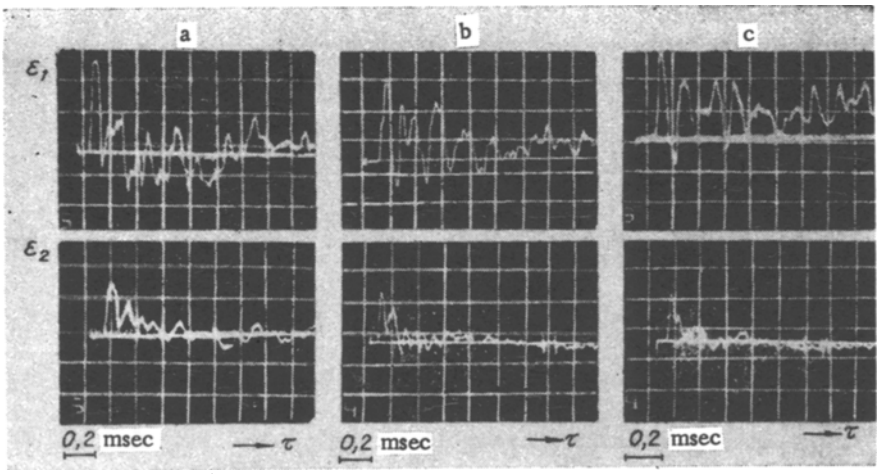

Fig. 4

the investigated range of thickness of the liquid filler, where ε_1 and ε_2 are the mean values of these amplitudes in the internal and external shells; $\varkappa = \varepsilon_1/\varepsilon_2$ is a coefficient expressing the nonuniformity of the strain distribution by shell layer ($\bar{\varepsilon}_1$, $\bar{\varepsilon}_2$, $\bar{\varkappa}$ are defined below).

The results shown make it possible to conclude that the peak circumferential strains are relative slightly dependent on the thickness of the liquid layer.

Comparison of the oscillograms of pressure in the incident wave (Fig. 3) and the strains (Fig. 4) shows that the secondary shocks have only a slight effect of shell vibration. Characteristic inflection points appear on the strain oscillograms of both the internal and external layers as a result of the action of the second impulse (the time of arrival of the front from the moment that shell motion begins is about 0.15 msec), but there is no increase in the maximum amplitudes of the vibrations here. The amplitudes of the third and fourth impulses are significantly less than the amplitude of the first impulse (the times of arrival are 0.35 and 0.56 msec, respectively), and no appreciable effects connected with them are seen.

The experimental results provide evidence of the appreciable nonuniformity of the strain distribution in the bearing layers: ε_1 is about 1.4-1.6 times greater than ε_2. Meanwhile, the nonuniformity coefficient $\varkappa$ decreases with an increase in H. This finding contradicts the theoretical data obtained with the assumption of cophasal motion of the shell layers during the first half-period of joint vibrations. Rough estimates of ε_1 and ε_2 give an approximate model of a single-layer shell of radius R_1 with equivalent stiffness K_e and inertial m_e characteristics [9]:

$$K_e = \frac{1}{R_1}\left[\frac{E}{1-\nu^2}\left(\frac{h_1}{R_1}+\frac{h_2}{R_2}\right)+\frac{K_0 H}{R_0}\right],$$

$$m_e = \frac{1}{R_1}\left[\rho\left(h_1 R_1 + h_2 R_2\right)+\rho_0 H R_0\right],$$

TABLE 1

H, mm	$\varepsilon_1 \cdot 10^4$	$\delta(\varepsilon_1)$	$\varepsilon_2 \cdot 10^4$	$\delta(\varepsilon_2)$	$\varkappa$	$\bar{\varepsilon}_1 \cdot 10^4$	$\bar{\varepsilon}_2 \cdot 10^4$	$\bar{\varkappa}$
27	13,2	1,21	8,3	0,39	1,58	14,0	8,9	1,58
47	11,2	1,20	7,6	0,39	1,47	12,7	6,2	2,04
77	10,1	3,41	7,3	0,38	1,38	11,8	4,2	2,84

$$\omega_0 = \frac{1}{2\pi}\sqrt{\frac{K_e}{m_e}}, \quad R_0 = \frac{R_1 + R_2}{2}, \tag{1}$$

where E, ν, and ρ are the Young's modulus, Poisson's ratio, and density of the material of the shells; K_0 and ρ_0 are the compressive bulk modulus and density of the liquid; ω_0 is the frequency of radial vibrations of the equivalent single-layer shell.

In accordance with (1), ω_0 = 4.96, 4.18, and 3.43 kHz (in order of increasing H) for the structures tested. If the characteristic time of action of the main part of the impulse of the external shock wave is shorter than one-fourth of the period of the natural vibrations of the shell ($\tau_* < T/4$, $T = \omega_0^{-1}$), then by making the initial velocity of the equivalent shell proportional to the pressure pulse [2] $\dot{w}_e = I/m_e$ we obtain a simple formula to evaluate the strain ε_1 of the equivalent one-layer shell:

$$\varepsilon_1(t) = \bar{\varepsilon}_1 \sin(2\pi\omega_0 t), \quad \bar{\varepsilon}_1 = I/(2\pi m_e \omega_0 R_1). \tag{2}$$

Assuming the layer of liquid between the shells to be incompressible, we find the strain of the external shell

$$\varepsilon_2(t) = \bar{\varepsilon}_2 \sin(2\pi\omega_0 t), \quad \bar{\varepsilon}_2 = (R_1/R_2)^2 \bar{\varepsilon}_1. \tag{3}$$

Values of $\bar{\varepsilon}_1$, $\bar{\varepsilon}_2$, and $\bar{\varkappa} = \bar{\varepsilon}_1/\bar{\varepsilon}_2$ calculated from (2) and (3) are shown in Table 1 for the system and loading parameters used in the experiment. The maximum strains of the equivalent shell $\bar{\varepsilon}_1$ turned out to agree quite well with the data obtained experimentally for the inside layer. At the same time, comparison of the experimental oscillograms and solution of (2) shows that it is necessary to allow for the higher vibration modes of the system. These modes could have been calculated analytically (by using a model with many degrees of freedom) and a parametric analysis could then have been performed. However, as was shown in [9], it proved to be more efficient and basically as convenient to model the nonsteady deformation of a three-layer shell of the type in question numerically on a computer.

The system of differential equations of axisymmetric hydroelasticity was calculated simultaneously on a BÉSM-6 computer with the use of an explicit finite-difference scheme. The motion of the liquid is described by a unidimensional wave equation for the velocity potential φ, while the motion of the shell is described by equations of the dynamics of a thin circular ring:

$$\frac{\rho}{E}\ddot{w}_1 = -\frac{w_1}{R_1^2} - \frac{p_1 - p_0}{h_1 E}, \quad \frac{\rho}{E}\ddot{w}_2 = -\frac{w_2}{R_2^2} + \frac{p_2}{h_2 E},$$
$$\frac{\ddot{\varphi}}{c_0^2} = \frac{1}{r}\frac{\partial\varphi}{\partial r} + \frac{\partial^2\varphi}{\partial r^2} \quad (R_1 \leqslant r \leqslant R_2), \quad c_0^2 = \frac{K_0}{\rho_0}, \tag{4}$$
$$p_1 = -\rho_0 \left.\frac{\partial\varphi}{\partial t}\right|_{r=R_1}, \quad p_2 = -\rho_0 \left.\frac{\partial\varphi}{\partial t}\right|_{r=R_2},$$

where w_1 and w_2 are displacements of the inside and outside shells; c_0 is the speed of sound in the liquid. We took zero initial conditions. The boundary conditions on the wetted surfaces correspond to equality of the normal velocities of the shells and liquid:

$$\left.\frac{\partial\varphi}{\partial r}\right|_{r=R_1} = \dot{w}_1, \quad \left.\frac{\partial\varphi}{\partial r}\right|_{r=R_2} = \dot{w}_2. \tag{5}$$

Equations (4), with boundary conditions (5), correspond to an exact model of hydroelasticity in a linear formulation. The parameters of the shock wave incident on the internal shell p_0 corresponded to the experimentally measured values (see Fig. 3).

To make the numerical calculations more accurate, the parameters of the difference grid were chosen so as to minimize numerical dispersion [10]. More detailed information on the method of calculation used and features of finite-difference algorithmization of nonsteady hydroelasticity problems is contained in [9, 11].

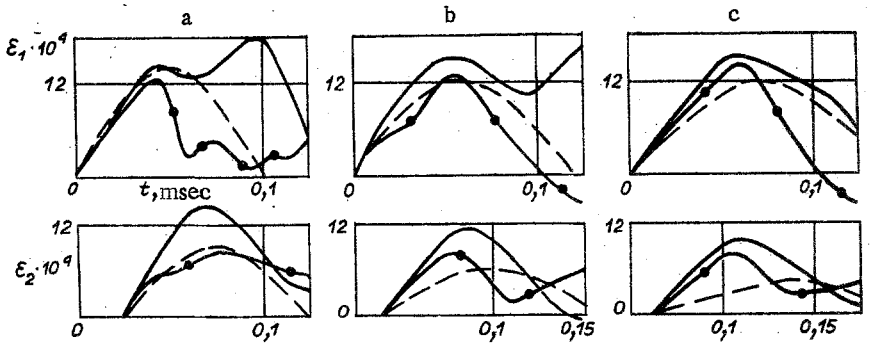

Fig. 5

Figure 5a-c shows oscillograms of the radial strains ε_1 and ε_2 for H = 27, 47, and 77 mm. The solid curves represent results calculated by the exact theory, the dashed curves show results obtained from simplified model (2-3), and the curves with points show the experimental data.

Analysis of the curves $\varepsilon_1(t)$ showed that the theoretical and experimental data agree fairly well within the time interval $0 < t \lesssim T/4$, where the strains are maximal. The strain oscillograms calculated from the approximate and exact theories nearly coincide up to $t = 0.65 \cdot 10^{-4}$ sec for the system with the smallest gap (H = 27 mm). This value of t is almost twice as great as the time of travel of an acoustic wave over the distance 2H. The approximate theory gives understated (by about 15%) amplitudes for other values of H, but the qualitative character of the oscillograms remains the same up to $t = 3H/c_0$ (H = 47 mm) and $t = 2.5H/c_0$ (H = 77 mm). Thus, the function $\varepsilon_1(t)$ can be evaluated with a reliability adequate for practical purposes by Eq. (2) in the interval $0 < t \lesssim T/4$.

The oscillograms of strains in the external shell $\varepsilon_2(t)$ obtained in the experiment are described well by approximate equation (3) only in the case H = 27 mm. The agreement between the results obtained from the approximate model and the experiment becomes poorer with an increase in H, and at H = 77 the maximum amplitude and frequency of $\varepsilon_2(t)$ is almost half the experimental values. Conversely, the exact theory gives an overstated amplitude, and the agreement between this theory and the experiment is poorest at H = 27 mm.

The above comparisons show that insofar as describing the functions $\varepsilon_1(t)$ and $\varepsilon_2(t)$ obtained experimentally are concerned, the exact model of linear hydroelasticity does not offer any advantages over the approximate model of an equivalent system with one degree of freedom. It thus becomes clear that the significant difference in the behavior of the experimental and theoretical oscillograms at $t > T/4$ is due to causes other than whether or not allowance is made for the higher vibration modes in the linear hydroelasticity model. One of these causes is the lack of correspondence between the linear strain model of an ideal liquid and the experimentally studied process. In the experiment, the resistance of the liquid to compression is quite different from its resistance to tension.

Figure 6 shows the pressure acting on the external shell from the direction of the liquid layer (the solid curves show theoretical results, the curves with points show experimental results; H = 27 and 77 mm in a and b). The leading pressure pulses (compression phase) are in good agreement. The linear theory establishes a rarefaction phase after the compresssion, and henceforth positive and negative phases alternate. No rarefaction phases were observed in the experiment. The appearance of the oscillograms suggests that the liquid may separate from the walls (and possibly within the layer) when the rarefaction pressure reaches certain (relatively small) amplitudes. Such separation leads to cavitation and oscillations in the liquid which are quite nonlinear. As a result, the continuity of the liquid is disturbed, and the connection between the shells becomes indeterminate. This is not considered by the linear model of hydroelasticity on which the calculations were based, and the results obtained with this model cease to reflect the actual process at the moment the pressure reaches negative values.

The intensity decay of free vibrations noted in the tests is evidently connected with cavitation. Thus, from the point of view of the strength of the shells, the occurrence of nonlinear processes in a liquid undergoing cavitation may be useful when the shells are subjected to repeated loading in service (such as in blast chambers).

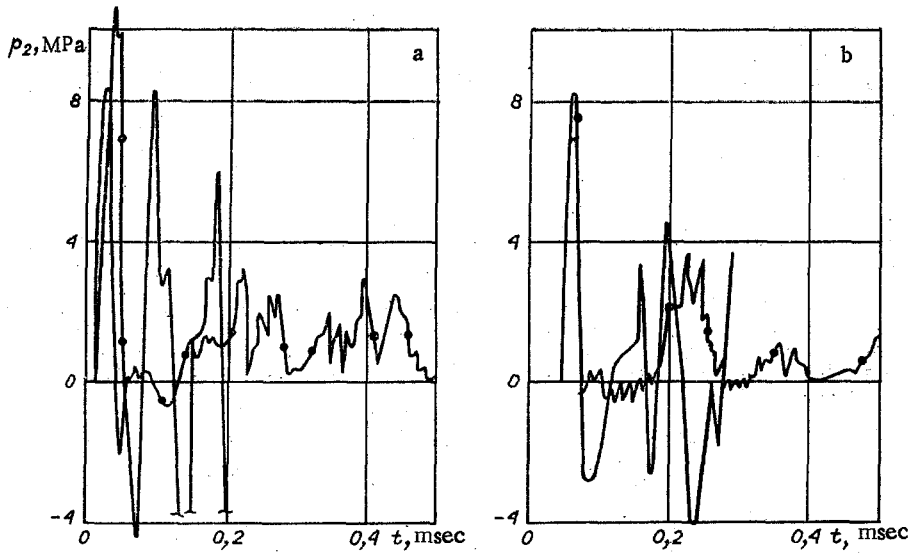

Fig. 6

No significant changes were seen in the general character of vibrations with an increase in the thickness of the liquid layer. There were only certain differences in the details of the processes. In particular, there was a tendency for the vibrations to decay more slowly with an increase in H on the inside layer and for the opposite to occur on the outside layer — where the vibration process became aperiodic at H = 77 mm. The reason for these changes is weakening of the interaction of the layers as a result of an increase in the distance between them.

Apart from the central zone of the shell, it is interesting to note the strain in the region of edge effects — at the joints between the shell and the rigid flanges. No concentration of dynamic strains was seen here. In particular, the maximum transverse and circumferential strains recorded by gauges 1 and 2 near the flanges on the surface of the external bearing layer with H = 47 mm were $5.2 \cdot 10^{-4}$ and $2.1 \cdot 10^{-4}$.

In conclusion, we should note that an estimate of the maximum circumferential strains (with the error in the safety factor) can be obtained by calculation from the linear model of hydroelasticity. The strains of the most heavily loaded internal layer can be determined with an accuracy sufficient for practical purposes from the approximate model of the system as a body with one degree of freedom.

We thank Sh. U. Galiev and A. F. Demchuk for their useful discussions.

LITERATURE CITED

1. A. F. Demchuk, Metal Blast Chambers [in Russian], Inst. Gidrodin. Sib. Otd. Akad. Nauk SSSR, Novosibirsk (1968).
2. A. F. Demchuk, "Method of designing blast chambers," Zh. Prikl. Mekh. Tekh. Fiz., No. 5 (1968).
3. A. G. Ivanov, S. A. Novikov, and V. A. Sinitsyn, "Study of the behavior of closed steel shells with the detonation of explosive charges in them," Zh. Prikl. Mekh. Tekh. Fiz., No. 6 (1968).
4. V. V. Adishchev and V. M. Kornev, "Design of shells for blast chambers," Fiz. Goreniya Vzryva, 15, No. 6 (1979).
5. V. M. Kornev, V. V. Adishchev, et al., "Experimental study and analysis of vibrations of the shell of a blast chamber," Fiz. Goreniya Vzryva, 15, No. 6 (1979).
6. A. A. Buzukov, "Features of the behavior of the walls of blast chambers under the influence of a shock load," Fiz. Goreniya Vzryva, 12, No. 4 (1976).
7. A. A. Buzukov, "Loads created by explosions in an air-filled blast chamber," Fiz. Goreniya Vzryva, 16, No. 5 (1980).
8. R. Cenerini, S. Curioni, H. Holtbecker, et al., "Experimental analysis of composed structure subject to a dynamic load," in: Proc. of the First Int. Conf. Struct. Mech. React. Technol., Vol. 3, Berlin (1971).
9. N. I. Pinchukova, "Dynamics of two coaxial cylindrical shells with a liquid filler," Submitted to VINITI, No. 4677-82 DEP, IGD Sib. Otd. Akad. Nauk SSSR, Novosibirsk (1982).

10. M. V. Stepanenko, "Method of calculating nonsteady impulsive strain processes in elastic structures," FTPRPI, No. 2 (1976).
11. N. I. Pinchukova and M. V. Stepanenko, "Action of an acoustic pressure wave on a shell of revolution," Submitted to VINITI, No. 2287-82 DEP, IGD Sib. Otd. Akad. Nauk SSSR, Novosibirsk (1982).

ELASTIC–PLASTIC STATE OF A WEDGE WITH LIMITING RESISTANCE TO SHEAR AND SEPARATION

I. T. Artem'ev and D. D. Ivlev

UDC 539.375

The equilibrium of an acute-angled wedge is examined under plane strain conditions under the action of a uniformly distributed load q applied along the normal to one of its faces (Fig. 1) in the presence of strength limits $k > 0$, $d > 0$ to shear and separation [1] such that the tangential and normal stress components would satisfy the conditions $\tau_{max} \leqslant k$, $\sigma_{max} \leqslant d$. The domain in which the maximal stress components do not reach these limits will be considered elastic.

In contrast to an elastic–plastic wedge (with a limiting resistance to just shear [2]), in this case the size of the limit state zone depends on not only the magnitude but also the direction of the load ($q > 0$, $q < 0$). Intervals of the load q that correspond to different qualitative states of the wedge are determined.

1. In the general case the wedge is separated into three zones I–III (Fig. 1) in which shear, elastic, and separation states, respectively, occur. The equations for the stress in zone I are of hyperbolic type and have two orthogonal families of rectilinear characteristics inclined to the free boundary at the angle $\pi/4$, while the equations in zone III are of parabolic type and have one family of characteristics orthogonal to the principal stress [1]. A uniform stressed state is realized in zones I and III and the boundaries with zone II are rectilinear.

Let us ascribe the superscripts minus and plus, respectively, to the stress tensor components in zones I and III. Here the principal stresses have the definite values

$$\sigma_1^- = 0, \quad \sigma_2^- = -2k, \quad \sigma_1^+ = d, \quad \sigma_2^+ = -q.$$

The stress states in zones I and III are interpreted by Mohr diagrams in Fig. 2. The normal and tangential stress tensor components can evidently be defined in terms of the principal stresses on the lines OB and OC separating the three zones and making the angles α and β with the wedge faces (see Fig. 1). We have in the r, θ polar coordinates

$$\sigma_\theta^-, \sigma_r^- = k(\pm\cos 2\alpha - 1), \quad \tau_{r\theta}^- = k\sin 2\alpha, \quad \sigma_\theta^+, \sigma_r^+ = p \mp \rho\cos 2\beta, \quad \tau_{r\theta}^+ = \rho\sin 2\beta, \tag{1.1}$$

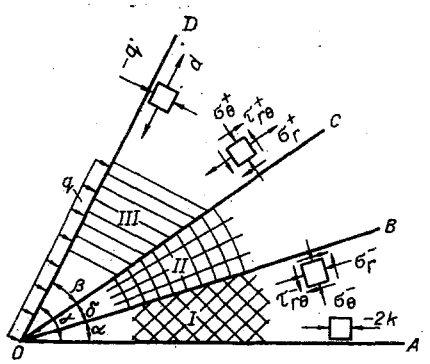

Fig. 1

Cheboksary. Translated from Zhurnal Prikladnoi Mekhaniki i Tekhnicheskoi Fiziki, No. 1, pp. 157–161, January–February, 1986. Original article submitted September 21, 1984.

